

1 **Supporting Information for:**

2

3 **Grazing strategies determine the size composition of phytoplankton in**

4 **eutrophic lakes**

5

6

7 Sze-Wing To<sup>1,2,\*</sup>, Esteban Acevedo-Trejos<sup>2,3</sup>, Subhendu Chakraborty<sup>2</sup>, Francesco Pomati<sup>4,5</sup>, Agostino

8 Merico<sup>2,1</sup>

9

*<sup>1</sup> School of Science, Constructor University, Bremen, Germany*

*<sup>2</sup> Department of Integrated Modelling, Leibniz Centre for Tropical Marine Research (ZMT), Bremen, Germany*

*<sup>3</sup> Earth Surface Process Modelling, German Research Centre for Geoscience (GFZ), Potsdam, Germany*

*<sup>4</sup> Aquatic Ecology, Swiss Federal Institute of Aquatic Science and Technology (Eawag), Dübendorf, Switzerland*

*<sup>5</sup> Institute of Integrative Biology, ETH, Zurich, Switzerland*

10

11 \* Corresponding Author: Sze-Wing To [sto@constructor.university](mailto:sto@constructor.university)

12

13

14

## 15 **Supporting Information S1 - Environmental forcing to the model and model applications**

16

17 The three environmental forcing applied to the model are lake water surface temperature (LWST),  
18 photosynthetically active radiance (PAR), and mixed layer depth (MLD) (Fig. S1). The former two  
19 forcing functions are based on the projection data of temperate lakes in 40°N adopted from Layden et al.  
20 (2015). The three yearly mixing regimes (i.e. constant, medium and high frequencies) applied to the  
21 model was obtained theoretically from a sinusoidal function as following:

22

### **Mixing regimes**

### **Sinusoidal functions**

Constant  
(no mixing throughout the year)

-

Medium frequency  
(4 mixings per year)

$$\left( \frac{(Z_m - Z_t)}{2} + Z_t \right) + \frac{(Z_m - Z_t)}{2} \cdot \cos\left( \frac{DoY}{14.525} \right)$$

High frequency  
(12 mixings per year)

$$\left( \frac{(Z_m - Z_t)}{2} + Z_t \right) + \frac{(Z_m - Z_t)}{2} \cdot \cos\left( \frac{DoY}{4.825} \right)$$

23

24 where

25  $Z_m$  = mixing depth (m), 80m in the study

26  $Z_t$  = thermocline depth (m), 2.5m in the study

27  $DoY$  = day of year

28

29 The data for LWST and PAR are digitalized with WebPlotDigitizer 4.2 (Rohatgi 2021) and are archived  
30 in the Github repository ([https://github.com/systemsecologygroup/Sizeb\\_NPZD](https://github.com/systemsecologygroup/Sizeb_NPZD)). The model is coded in  
31 Python (version 3.7.x). The simulations are performed using the *odeint* function in the *scipy* package  
32 (Virtanen et al. 2020).

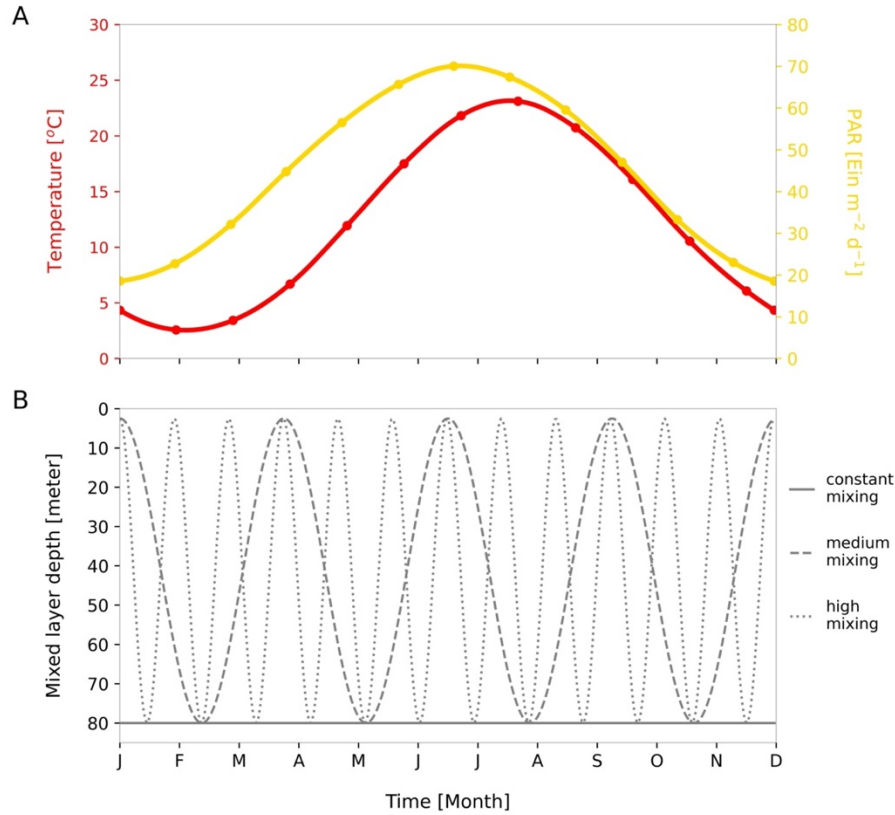


**Figure S1.** Temporal patterns of abiotic environmental forcing variables used in the model. (A) The red and yellow curves represent interpolated functions of annual variation in, respectively, temperature and photosynthetically active radiance (PAR, converted from net shortwave solar irradiance, W m<sup>-2</sup>). The dots symbolized the projection data adopted from Layden et al. (2015). (B) The functions represent three mixing frequencies: constant, medium, and high mixing frequencies – solid, dashed, and dotted line respectively, designed to test their effects on plankton dynamics. The integrated mixed layer depth ranges between 2.5 and 80 meters.

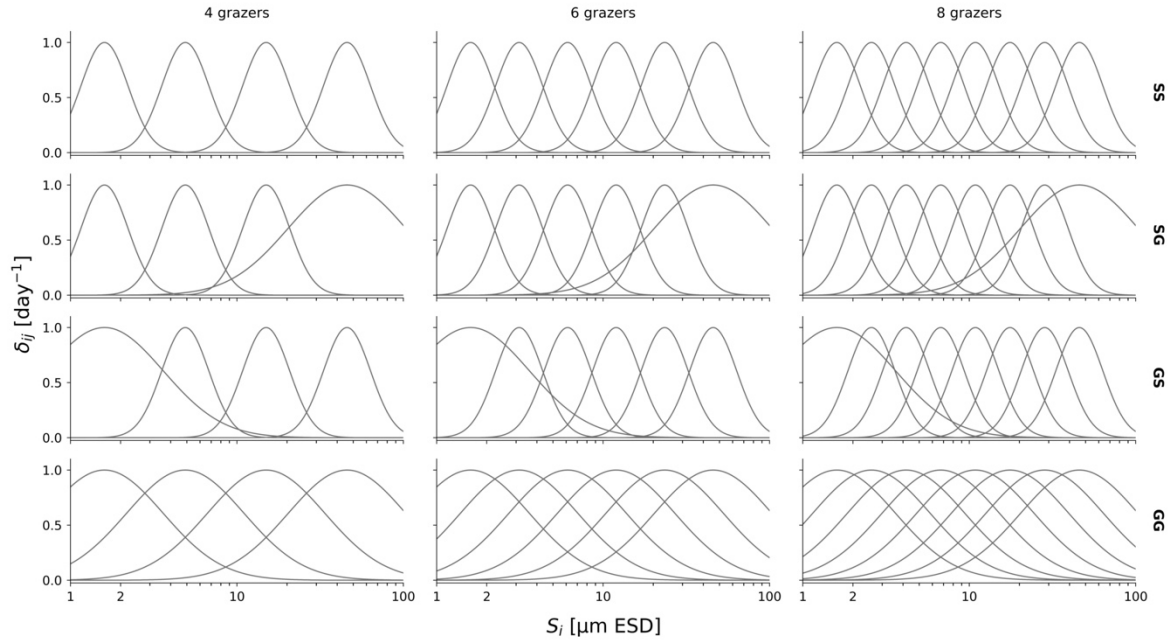
## 43    **Supporting Information S2 – Sensitivity analyses**

44    Phytoplankton size structure is highly responsive to zooplankton grazer community structure (Fuchs and  
45    Franks 2010; Prowe et al. 2012; Chenillat et al. 2021), to investigate the robustness of our results, we  
46    conduct a series of sensitivity analyses by varying the zooplankton community structure and the  
47    allometric scaling for growth and for grazing. All sensitivity analyses are simulated for different  
48    scenarios of grazing strategies i.e., “SS”; “SG”; “GS”; and “GG” (Fig. 3), and these analyses are  
49    simulated only for more perturbed environmental conditions i.e., non-oligotrophic condition with a  
50    presence of mixing — the combination of eutrophic or hypertrophic condition and medium or high  
51    mixing — in which the system is not predominately controlled by bottom-up processes and hence the  
52    effects of different grazing strategies are more pronounced.

### 53    *2.1    An increasing number of grazers and extended grazer size range*

54    We vary the number of grazers in the system for different scenarios of grazing strategy (Fig. 3A) by  
55    dividing proportionally the specialist and generalist grazers according to the scenario. For example, a 4-  
56    grazer “SG” case involves two specialist and two generalist grazers respectively; a 6-grazer “SG” case  
57    involves three specialist and three generalist grazers respectively; *vice versa* (Supplementary Fig. S2).  
58    Essentially, the assumption where the group of small phytoplankton are under heavier grazing pressure  
59    than their larger counterparts is held for all scenarios. We additionally extended the size range of  
60    zooplankton, capturing the grazing effect from nanozooplankton to microzooplankton (i.e., 5-2000  $\mu\text{m}$ ),  
61    such that their grazing covers the entire phytoplankton size spectrum in the model from 1 to 100  $\mu\text{m}$   
62    (Supplementary Fig. S2). The total number of phytoplankton size classes,  $i$ , is fixed to 150.

63



64

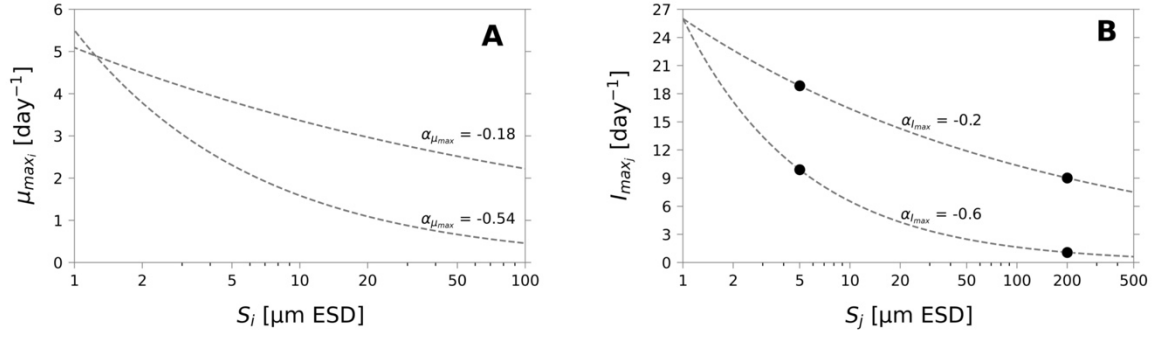
65 **Figure S2.** The configurations of sensitivity analyses for different zooplankton community structures. We vary the  
 66 number of grazers to four, six and eight (column-wise) for different grazing strategies. The zooplankton community  
 67 under all trophic structures are subject to a population-dependent predatory pressure (not shown in the illustration). The  
 68 maximum zooplankton size is extended to 2000  $\mu\text{m}$  where the grazing pressure covers the whole phytoplankton size  
 69 spectrum.

70

## 71 2.2 Different allometric scaling exponents

72 Allometric relationships that describe planktonic growth and grazing are substantial for understanding  
 73 selective pressure of phytoplankton community size structure (Taniguchi et al., 2014). The exponent of  
 74 these allometries have been in debate for decades, especially for phytoplankton maximum growth rate  
 75 and zooplankton maximum ingestion rates (e.g. Tang, 1995; Hansen et al., 1997; Saiz & Calbet, 2007;  
 76 Chen & Liu, 2010; DeLong et al., 2010; Edwards et al., 2012; Kempes et al., 2012; Mara  n et al., 2013;  
 77 Ward et al., 2017; Zaoli et al., 2019; Hillebrand et al., 2022). Poulin & Franks (2010) also commented  
 78 that any modelled trophic structure often depends on a specific set of allometric scaling relationships. To  
 79 confirm the consistency of our results, we simulated the phytoplankton community size structure under  
 80 different allometric relationships for the maximum growth rate,  $\mu_{max_i}$  (Eq. 3), and the maximum  
 81 ingestion rate,  $I_{max_j}$  (Eq. 10), by altering their allometric exponents,  $\alpha_{\mu_{max}}$  and  $\alpha_{I_{max}}$  respectively, for  
 82  $\pm 50\%$  (Supplementary Fig. S3). The tested values for  $\alpha_{\mu_{max}}$  are -0.54 and -0.18 and for  $\alpha_{I_{max}}$  are -0.6

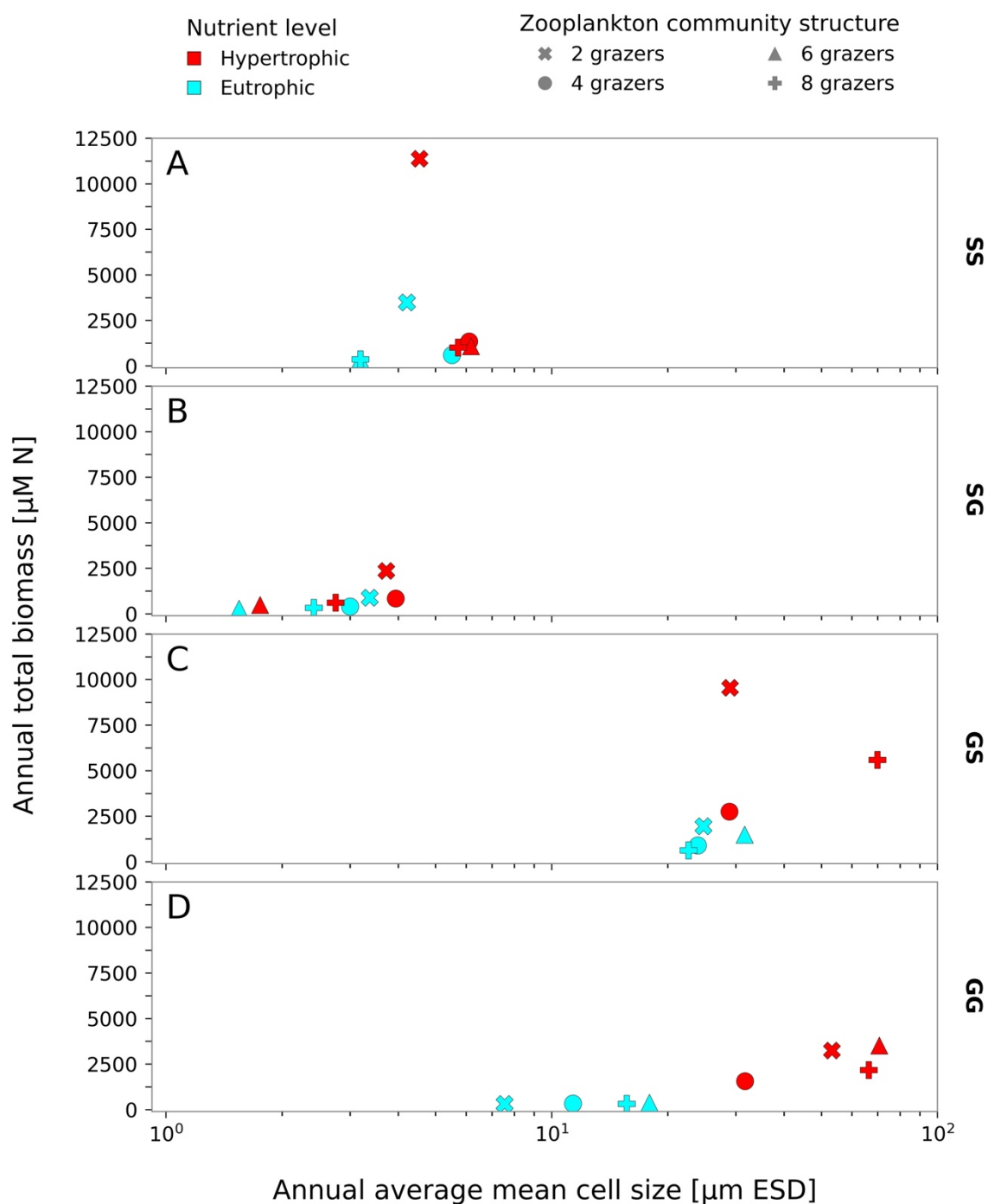
83 and -0.2. Here, a smaller  $\alpha_{\mu_{max}}$  and  $\alpha_{I_{max}}$  generally lead to a decrease in  $\mu_{max_i}$  and  $I_{max_j}$  to the  
 84 community but the decrease is less for smaller than large size classes (Supplementary Fig. S3). This leads  
 85 to a lower  $\alpha_{\mu_{max}}$  favours small cells over large in terms of the less reduction in growth ability whereas a  
 86 lower  $\alpha_{I_{max}}$  disfavours small over large in terms of the less reduction in grazing pressure.



87  
 88 **Figure S3.** Sensitivity analyses for allometric scaling of (A) maximum growth rate,  $\mu_{max_i}$ , and (B) maximum ingestion  
 89 rates,  $I_{max_j}$ , via varying the parameters,  $\alpha_{\mu_{max}}$  and  $\alpha_{I_{max}}$ ,  $\pm 50\%$  of their default values respectively.  $S_i$  and  $S_j$  are the  
 90 size of phytoplankton class  $i$  and zooplankton class  $j$  respectively.

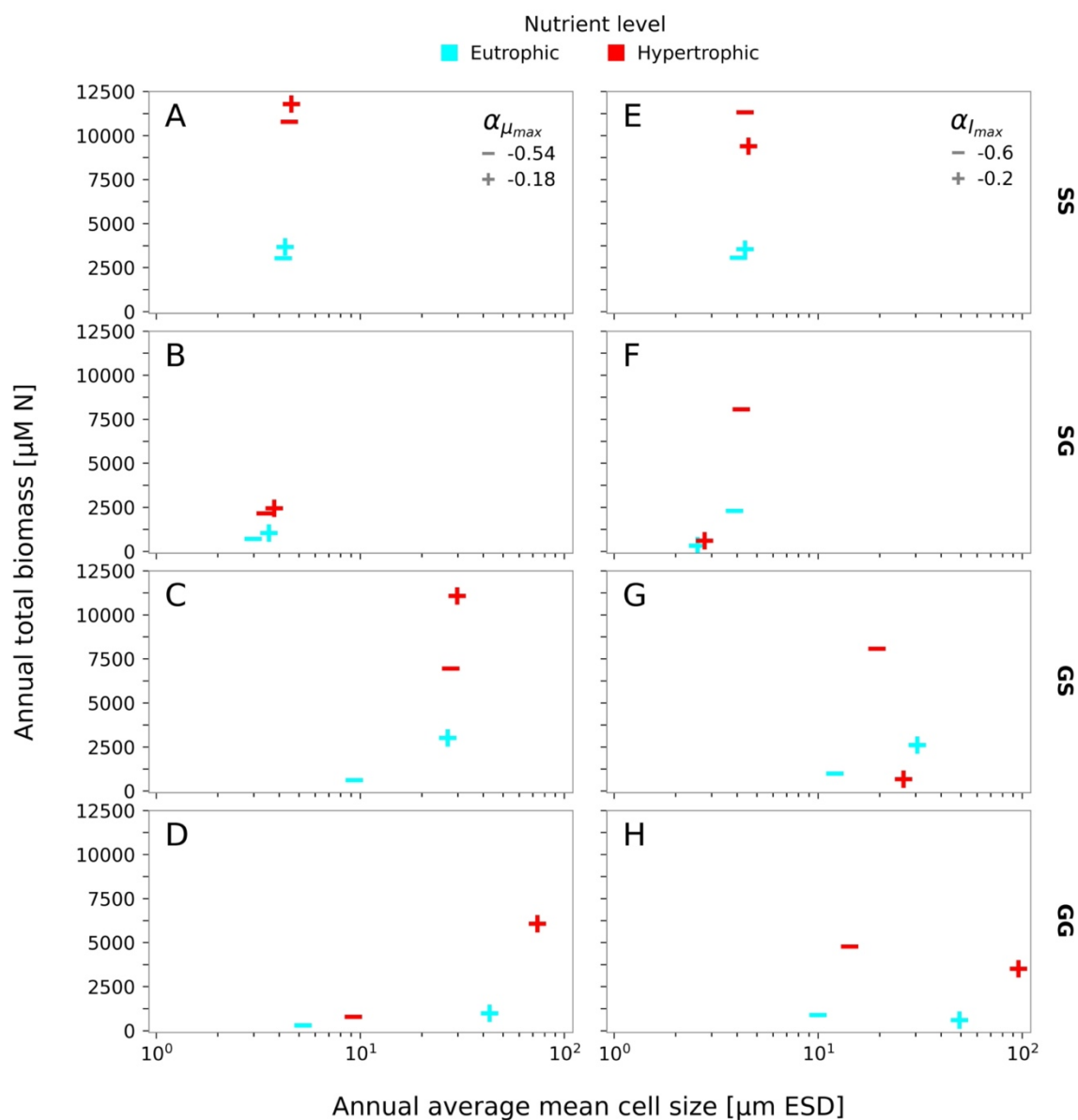
91 **Supporting Information S3 – Results of sensitivity analyses**

92 **3.1 The results for sensitivity analyses varying zooplankton community structure**



93

94 **Figure S4.** Annual biomass versus mean size under different grazing strategies and different nutrient conditions for  
 95 different community structure of zooplankton (symbolizations). For these runs, the mixing frequency is fixed to medium.



97

98 **Figure S5.** Annual biomass versus mean size for different (A-D)  $\alpha_{\mu_{max}}$  and (E-H)  $\alpha_{I_{max}}$  under different grazing  
99 strategies and different nutrient conditions. For these runs, the mixing frequency is fixed to medium.

100

101



102 **Supplementary Table 1.** Description of parameters used in the model along with corresponding symbols, values, units,  
103 and literature sources.

Symbol	Description	Value	Unit	Source
$P_{max}$	Maximum photosynthesis rate	1.1	$d^{-1}$	this study
$\alpha_{P_I}$	Initial slope of the P-I curve	0.15	$Ein\ m^{-2}\ d^{-1}$	this study
$K_{par}$	Light attenuation coefficient	0.1	$m^{-1}$	Fasham et al. (1990)
$\omega$	Cross-thermocline mixing coefficient	0.1	$m\ d^{-1}$	Fasham et al. (1990)
$N_0$	Scenarios of nutrient supplied from the bottom water layer	1, 15, 50	$\mu M\ N$	this study
$\phi_P$	Natural mortality – phytoplankton	0.2	$d^{-1}$	this study
$\phi_Z$	Natural mortality – zooplankton	0.1	$d^{-1}$	this study
$\eta_Z$	Higher-order mortality rate – zooplankton	0.34	$d^{-1}$	Oschlies & Schartau (2005)
$\varepsilon$	Sloppy feeding	0.69	-	Fasham et al. (1990)
$\gamma$	Assimilation efficiency	0.75	-	Oschlies & Schartau (2005)
$\varphi$	Remineralisation rate	0.6	$d^{-1}$	this study
$K_p$	Half-saturation constant – zooplankton	3	$\mu M\ N$	this study
$\theta_j$	Prey size tolerance	0.2 (specialis t) 0.5 (generalis t)	$\mu m\ ESD$	Banas (2011), Hansen et al. (1994)

Symbol	Description	Value	Unit	Source
$S_i$	Cell sizes – phytoplankton	1-100	μm ESD	this study
$S_{Z_j}$	Body sizes – zooplankton	5 ( $Z_1$ ) 200 ( $Z_2$ )	μm ESD	this study
$\beta_{\mu_{max}}$	Intercept of allometric relationship for $\mu_{max_i}$	$10^{0.69}$	d <sup>-1</sup>	Edwards et al. (2012)
$\alpha_{\mu_{max}}$	Exponent of allometric relationship for $\mu_{max_i}$	-0.36	-	Edwards et al. (2012)
$\beta_{K_N}$	Intercept of allometric relationship for $K_{N_i}$	$10^{-0.71}$	μM N	Edwards et al. (2012)
$\alpha_{K_N}$	Exponent of allometric relationship for $K_{N_i}$	0.52	-	Edwards et al. (2012)
$\beta_{I_{max}}$	Intercept of allometric relationship for $I_{max_j}$	26	d <sup>-1</sup>	Hansen et al. (1997)
$\alpha_{I_{max}}$	Exponent of allometric relationship for $I_{max_j}$	-0.4	-	Hansen et al. (1997)
$\beta_{P_{opt}}$	Intercept of allometric relationship for $P_{opt_j}$	0.65	μm ESD	Hansen et al. (1997)
$\alpha_{P_{opt}}$	Exponent of allometric relationship for $P_{opt_j}$	0.56	-	Hansen et al. (1997)
$N_0, P_0, Z_0, D_0$	Initial conditions for all state variables	0.01	μM N	this study

104

105

106

107 **Reference**

- 108 Banas, N. S. 2011. Adding complex trophic interactions to a size-spectral plankton model: Emergent  
109 diversity patterns and limits on predictability. *Ecol. Model.* **222**: 2663–2675.  
110 doi:10.1016/j.ecolmodel.2011.05.018
- 111 Chen, B., and H. Liu. 2010. Relationships between phytoplankton growth and cell size in surface  
112 oceans: Interactive effects of temperature, nutrients, and grazing. *Limnol. Oceanogr.* **55**: 965–  
113 972. doi:10.4319/lo.2010.55.3.0965
- 114 Chenillat, F., P. Rivière, and M. D. Ohman. 2021. On the sensitivity of plankton ecosystem models to  
115 the formulation of zooplankton grazing E. Gorokhova [ed.]. *PLOS ONE* **16**: e0252033.  
116 doi:10.1371/journal.pone.0252033
- 117 DeLong, J. P., J. G. Okie, M. E. Moses, R. M. Sibly, and J. H. Brown. 2010. Shifts in metabolic  
118 scaling, production, and efficiency across major evolutionary transitions of life. *Proc. Natl.*  
119 *Acad. Sci.* **107**: 12941–12945. doi:10.1073/pnas.1007783107
- 120 Edwards, K. F., M. K. Thomas, C. A. Klausmeier, and E. Litchman. 2012. Allometric scaling and  
121 taxonomic variation in nutrient utilization traits and maximum growth rate of phytoplankton.  
122 *Limnol. Oceanogr.* **57**: 554–566. doi:10.4319/lo.2012.57.2.0554
- 123 Fasham, M. J. R., H. W. Ducklow, and S. M. McKelvie. 1990. A nitrogen-based model of plankton  
124 dynamics in the oceanic mixed layer. *J. Mar. Res.* **48**: 591–639.  
125 doi:10.1357/002224090784984678
- 126 Fuchs, H., and P. Franks. 2010. Plankton community properties determined by nutrients and size-  
127 selective feeding. *Mar. Ecol. Prog. Ser.* **413**: 1–15. doi:10.3354/meps08716
- 128 Hansen, B., P. K. Bjørnsen, and P. J. Hansen. 1994. The size ratio between planktonic predators and  
129 their prey. *Limnol. Oceanogr.* **39**: 395–403. doi:10.4319/lo.1994.39.2.0395
- 130 Hansen, P. J., P. K. Bjørnsen, and B. Hansen. 1997. Zooplankton grazing and growth: Scaling within  
131 the 2-2,000um body size range. *Limnol. Oceanogr.* **42**: 687–704.

132 Hillebrand, H., E. Acevedo-Trejos, S. D. Moorthi, A. Ryabov, M. Striebel, P. K. Thomas, and M.  
 133 Schneider. 2022. Cell size as driver and sentinel of phytoplankton community structure and  
 134 functioning. *Funct. Ecol.* **36**: 276–293. doi:10.1111/1365-2435.13986

135 Kempes, C. P., S. Dutkiewicz, and M. J. Follows. 2012. Growth, metabolic partitioning, and the size of  
 136 microorganisms. *Proc. Natl. Acad. Sci.* **109**: 495–500. doi:10.1073/pnas.1115585109

137 Layden, A., C. Merchant, and S. MacCallum. 2015. Global climatology of surface water temperatures  
 138 of large lakes by remote sensing: Global climatology of Lake Surface Water Temperatures. *Int.*  
 139 *J. Climatol.* **35**: 4464–4479. doi:10.1002/joc.4299

140 Marañón, E., P. Cermeño, D. C. López-Sandoval, T. Rodríguez-Ramos, C. Sobrino, M. Huete-Ortega,  
 141 J. M. Blanco, and J. Rodríguez. 2013. Unimodal size scaling of phytoplankton growth and the  
 142 size dependence of nutrient uptake and use G. Fussmann [ed.]. *Ecol. Lett.* **16**: 371–379.  
 143 doi:10.1111/ele.12052

144 Oschlies, A., and M. Schartau. 2005. Basin-scale performance of a locally optimized marine ecosystem  
 145 model. *J. Mar. Res.* **63**: 335–358. doi:10.1357/0022240053693680

146 Poulin, F. J., and P. J. S. Franks. 2010. Size-structured planktonic ecosystems: constraints, controls and  
 147 assembly instructions. *J. Plankton Res.* **32**: 1121–1130. doi:10.1093/plankt/fbp145

148 Prowe, A. E. F., M. Pahlow, S. Dutkiewicz, M. Follows, and A. Oshlies. 2012. Top-down control of  
 149 marine phytoplankton diversity in a global ecosystem model. *Prog. Oceanogr.* **101**: 1–13.  
 150 doi:10.1016/j.pocean.2011.11.016

151 Rohatgi, A. 2021. WebPlotDigitizer (version 4.2)[Computer software].

152 Saiz, E., and A. Calbet. 2007. Scaling of feeding in marine calanoid copepods. *Limnol. Oceanogr.* **52**:  
 153 668–675. doi:10.4319/lo.2007.52.2.0668

154 Tang, E. P. Y. 1995. The allometry of algal growth rates. *J. Plankton Res.* **17**: 1325–1335.  
 155 doi:10.1093/plankt/17.6.1325

156 Virtanen, P., R. Gommers, T. E. Oliphant, and others. 2020. SciPy 1.0: fundamental algorithms for  
157 scientific computing in Python. *Nat. Methods* **17**: 261–272. doi:10.1038/s41592-019-0686-2  
158 Ward, B. A., E. Marañón, B. Sauterey, J. Rault, and D. Claessen. 2017. The Size Dependence of  
159 Phytoplankton Growth Rates: A Trade-Off between Nutrient Uptake and Metabolism. *Am. Nat.*  
160 **189**: 170–177. doi:10.1086/689992  
161 Zaoli, S., A. Giometto, E. Marañón, and others. 2019. Generalized size scaling of metabolic rates based  
162 on single-cell measurements with freshwater phytoplankton. *Proc. Natl. Acad. Sci.* **116**: 17323–  
163 17329. doi:10.1073/pnas.1906762116  
164  
165  
166  
167  
168